

Assessment of Airframe Noise

P. J. W. Block*

NASA Langley Research Center, Hampton, Va.

A component method of airframe noise prediction is used to predict levels of operational and proposed aircraft airframe noise to assess the contribution of airframe noise to community noise levels. This is done after first evaluating the prediction method using newly acquired detailed measurements from full-scale aircraft and models. In the course of the evaluation, modeling techniques of airframe noise sources are examined with attention to scaling. Finally, when used to predict approach airframe EPNL's, the levels fell about 10 EPNdB below current noise regulations and about 5 EPNdB below proposed noise regulations.

Nomenclature

b_w	= wing span
C_1, C_2	= empirical constants in Eq. (2)
c	= ambient speed of sound
f	= frequency
f_m	= frequency of maximum predicted SPL
h	= airplane altitude
N	= parameter used in Eq. (1)
\bar{p}^2	= mean-square acoustic pressure
S_w	= wing area
V	= airspeed
δ_f	= trailing-edge flap deflection
δ_w	= boundary-layer thickness at the trailing edge of the wing
θ	= flyover angle
ϕ	= sideline angle
ν	= kinematic viscosity

Introduction

IN the past five years, much progress has been made in the area of airframe noise prediction. From the original attempts to predict the Overall Sound Pressure Level (OASPL) directly below conventional airplanes in the "clean" or cruise configuration, the art has progressed to predicting the OASPL in the "dirty" or landing configuration and, most recently, the noise spectrum and directivity of the individual airplane component noise sources. This latter development allows airframe noise prediction for airplanes with varying design as well as the calculation of subjective noise measures of an airplane overflight such as the Effective Perceived Noise Level (EPNL). Thus, one can achieve the ultimate goal of obtaining an estimate of the EPNL of airplanes of varying design to compare with noise regulations.

However, the accuracy of prediction methods is often in question since they have been generated and/or evaluated using only a limited data base, collected mostly from small conventional design airplane overflights. The airframe noise data base is particularly sparse in the area of supersonic aircraft airframe noise as well as sideline and flyover directivity measurements of conventional airplanes. To evaluate prediction methods, new data are required that are not already incorporated into the empirical base of the prediction schemes and that are detailed enough to test some of the assumptions that have been made.

Received Dec. 18, 1978; revision received May 24, 1979. This paper is declared a work of the U.S. Government and therefore is in the public domain. Reprints of this article may be ordered from AIAA Special Publications, 1290 Avenue of the Americas, New York, N.Y. 10019. Order by Article No. at top of page. Member price \$2.00 each, nonmember, \$3.00 each. **Remittance must accompany order.**

Index categories: Noise; Aeroacoustics.

*Aerospace Engineer, Acoustics and Noise Reduction Division. Member AIAA.

Recent detailed experimental studies of the airframe noise of full-scale aircraft and models provide the potential for evaluating prediction schemes in areas that heretofore were not possible. These data include sideline and flyover directivity measurements for conventional and supersonic design airframes. Thus, one purpose of this paper is to evaluate the accuracy of a reference airframe noise prediction method using the results of these detailed experimental studies. In the course of this evaluation, various assumptions that have been employed will be tested, scaling effects will be examined and some areas where understanding is still lacking will be highlighted. The second yet primary purpose of the paper is, in light of the evaluation, to use the prediction to estimate the airframe noise levels of operational and proposed aircraft and to compare these with noise regulations. Proposed aircraft considered are an energy efficient commercial transport (using laminar flow control), a proposed supersonic commercial transport, a spanloader transport, and the Space Shuttle.

Prediction Method

Although several airframe noise prediction methods have been proposed¹⁻³ the one developed by Fink⁴ for the Federal Aviation Administration will be evaluated here, since this method (which has been called the FAA method in Ref. 4) has recently been chosen as the reference airframe noise prediction by the Noise Prediction Task Force of the Working Group E under the Committee for Aircraft Noise of the International Civil Aeronautics Organization. The method models the individual components of the airframe (wing, flaps, tail, landing gear, etc.) as elementary sources or source distributions whose acoustic characteristics (spectra and directivity) have been derived analytically or empirically or have been assumed. The noise contribution from each of the components is then summed to obtain the total airframe noise. (In so doing, the effects of component interaction are ignored; however, the magnitude of most of these interactions has been found to be less than the accuracy of the prediction method.⁵) For example, the noise from the aircraft in the cruise configuration is a sum of the noise from the wing and the horizontal and vertical tail components. The noise from the other components (landing gear, leading-edge flaps and slats, and trailing-edge flaps) is added to the basic cruise configuration noise to obtain the noise of the landing configuration. The method was based empirically on the data from the VC-10, 747, Convair 990, and Jetstar among others. Comparisons with these aircraft and other details may be found in Ref. 4.

More precisely, this FAA method models the individual component noise sources as shown in Fig. 1. Noise generated by the clean wing is assumed to be wholly attributable to trailing-edge noise. The OASPL is derived semiempirically based on the work of Ffowcs-Williams and Hall⁶ and is given

by

$$\begin{aligned} \text{OASPL} = & 50 \log_{10} (V/c) + 10 \log_{10} [(\delta_w b_w)/h^2] \\ & + 8(N) + 20 \log_{10} (\cos^2 \phi \sin \theta \cos \theta / 2) + 143.5 \text{ dB} \end{aligned} \quad (1)$$

where N is a parameter set equal to zero for aerodynamically clean and to unity for aerodynamically dirty wing surfaces (such as those having complex flap assembly fairings, etc.). The angles θ and ϕ are the flyover and sideline angles (at the emission time) of the observer relative to the source axis and flyover plane, respectively (see Fig. 1). The convective amplification factor due to source motion was omitted from this empirical prediction scheme, since including it lessened the agreement with available data.

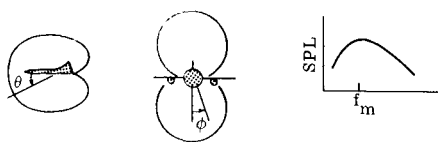
The spectral shape for clean airfoil shaped surfaces was estimated from a semiempirical study of blown flap noise and is given by

$$\text{SPL}_{1/3} - \text{OASPL} = 10 \log_{10} \{ C_1 (f/f_m)^4 [(f/f_m)^{C_2} + 0.05]^{-4} \} \quad (2)$$

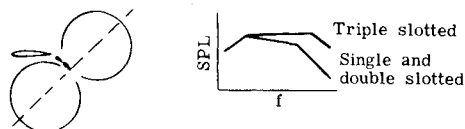
where $\text{SPL}_{1/3}$ is the one-third octave sound pressure level. Here $C_1 = 0.613$ and $C_2 = 1.5$ for conventional design wings where the taper ratio (ratio of wing chord at the tip to that at that root) is greater than $1/4$ and $C_1 = 0.485$ and $C_2 = 1.35$ for supersonic design wings where the taper ratio is less than $1/4$. The latter case was considered by Fink⁷ subsequent to the publication of Ref. 4. The frequency of maximum amplitude f_m is given by

$$f_m = 0.1V/\delta_w \quad (3)$$

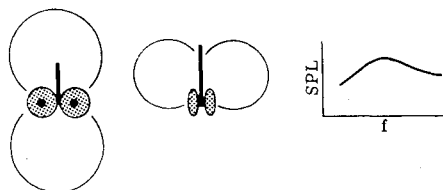
Wing and tail noise $\bar{p}^2 \sim V^5 \cos^2(\theta/2) \cos^2 \phi$



Trailing edge flap noise $\bar{p}^2 \sim V^6 \sin^2(\theta + \delta_F) \cos^2 \phi$



Landing gear noise $\bar{p}^2 \sim V^6 \sin^2 \phi \sin^2 \theta$



Leading edge slat noise $\bar{p}^2 \sim V^5 \cos^2(\theta/2) \cos^2 \phi$

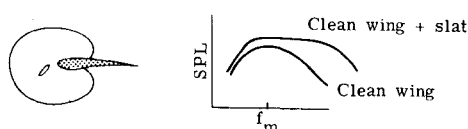


Fig. 1 Noise source models for the component method of airframe prediction.

where δ_w , the turbulent boundary-layer thickness, at the trailing edge, is given by

$$\delta_w = 0.37(S_w/b_w)(VS_w/b_w\nu)^{-1/5} \quad (4)$$

Equation (4) is simply the turbulent boundary-layer thickness at the mean aerodynamic chord at the Reynolds number based on the same streamwise dimension. The preceding equations are used to predict the noise from the clean wing as well as from other airfoil shaped surfaces such as the horizontal and vertical tail and leading-edge slats. The latter is modeled as an airfoil having a chord dimension which is 15% of the wing chord.

The noise from the trailing-edge flaps is assigned a dipole directivity which is oriented normal to the last flap segment (see Fig. 1). The spectrum is determined empirically from overflights of aircraft with single, double, and triple slotted flaps. Of note here is that the triple slotted flap is assigned more high-frequency content than the single and double slotted designs. Details may be found in Ref. 4.

The landing gear noise is modeled as the sum of two dipoles, one for the wake shed from the strut, and one for the wake shed by the wheels (see Fig. 1). Empirical relations for the noise were obtained using the results from an experimental investigation of model landing gear noise.⁸ Noise produced by wheel well cavities is assumed to be negligible at typical approach velocities based on the results of Ref. 9.

This FAA component method prediction scheme has been incorporated into the NASA Aircraft Noise Prediction Program (ANOPP) at the Langley Research Center.¹⁰ In addition to calculating the airframe noise via this method, ANOPP accounts for atmospheric attenuation, ground effects, aircraft rotation, and applies the Doppler correction to the predicted source frequency. This program was used to calculate the predicted levels of airframe noise via the FAA method for the various flight paths and configurations examined in this study.

Evaluation of Prediction

The FAA component prediction method will be evaluated using the results from several recent experimental studies of airframe noise, none of which were included in the data base from which the method evolved. Data on the DC-9 commercial airplane, two gliders, and three models have been utilized. These comparisons of predicted and measured levels are made at the observer (microphone) location except where noted. Atmospheric effects and ground effects are included where appropriate. Angles are corrected and given at the emission time with respect to the source axis for both flyover and model data. All model data have been corrected for background noise. Comparisons are made with the directivity and then the spectral data.

DC-9 Study

A recent detailed experimental study of the airframe noise of the DC-9¹¹ was carried out in which spectral and directivity data were obtained in a high signal-to-noise ratio environment. All data presented in this study were greater than 6 dB above the background noise levels. A typical cruise configuration and landing configuration flyover were selected from this study for comparison purposes.† Data were collected at several points directly under the flight path and at a 152.4-m (500-ft, 0.082-nm) and a 304.8-m (100-ft, 0.164-nm) sideline location for both of the overflights.

The measured and predicted directivity of the airframe noise at the flyover and sideline microphone locations are plotted in Fig. 2. For the cruise configuration (Fig. 2a), the agreement is reasonable with an rms variation of 1.1 dB in the flyover plane, 1.7 dB at the 152-m (500-ft) sideline position,

†These data were made available to the author through contract NAS1-14696 to the NASA Langley Research Center.

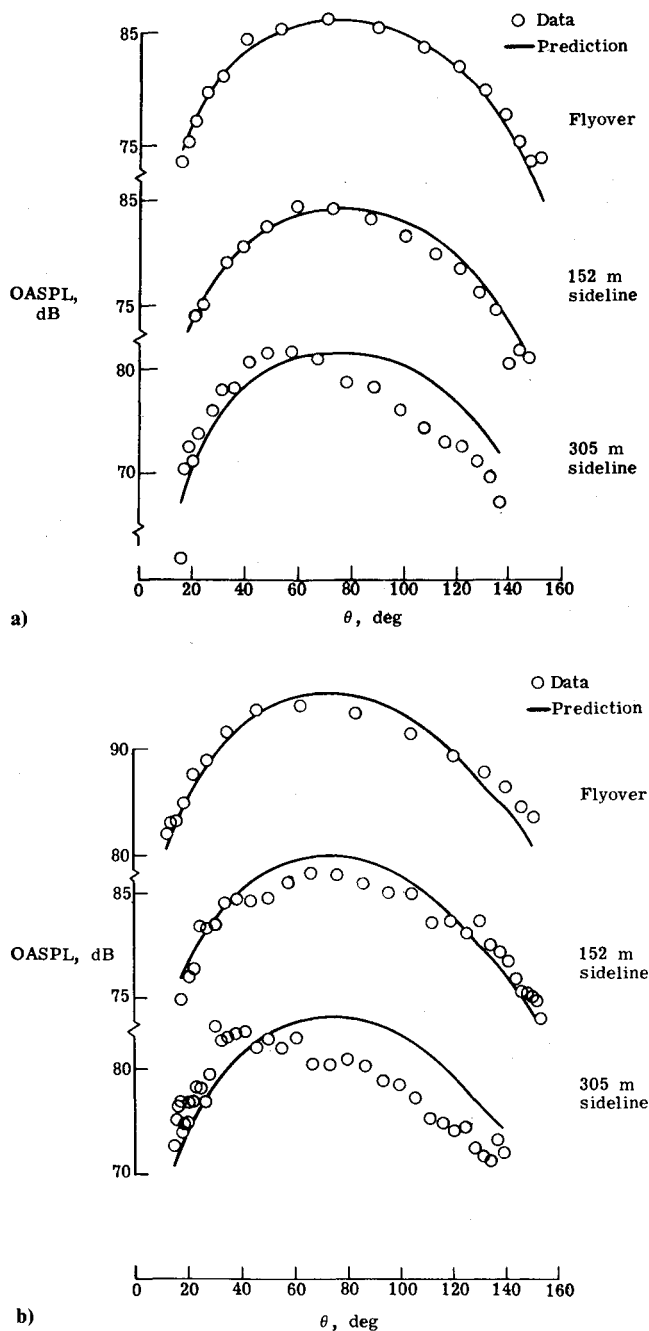


Fig. 2 Variation of the OASPL with the flyover angle θ for a DC-9 overflight: a) cruise configuration— $V = 151$ m/s, $h = 231$ m; b) landing configuration— $V = 91.2$ m/s, $h = 116$ m.

and 3 dB at the 305-m (1000-ft.) sideline position. The 304-m sideline data display an asymmetric behavior with the maximum OASPL occurring at 50 deg, considerably ahead of the predicted angle for the peak.

Similar agreement is seen for the landing configuration shown in Fig. 2b. The rms variations are 1.4, 1.6, and 3.7 dB for the flyover, 152-m, and 305-m positions, respectively. The same asymmetric behavior is observed in the 304-m sideline data for the landing configuration as was seen in the cruise configuration. This behavior is as yet unexplained; however, the lessening agreement with sideline angle does not affect the calculation of the EPNL, which is the ultimate goal of this study. It can, however, affect the calculation of a footprint.

Recall that the prediction method for the clean wing omits the convective amplification factor which theoretically should be present for a moving source. This omission tacitly assumes that the directivity of airframe noise is independent of Mach

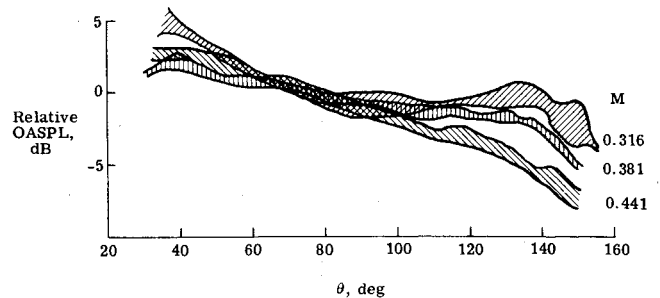


Fig. 3 Effect of Mach number on the airframe directivity in the cruise configuration.

number. The data, however, show a Mach number dependence as seen in Fig. 3. These data represent three overflights of the DC-9 in the cruise configuration at the three velocities listed on the figure. Each band in Fig. 3 represents the data (corrected to the source) measured by four microphones under the flight path. The data are normalized at 75 deg. (Such normalization is suggested by the form of the half-baffled dipole with convective amplification.) These data show a definite dependence of the directivity on Mach number, more in fact than can be attributed solely to the Doppler amplification factor. Thus, convective effects are evident. Unfortunately, this makes the good agreement for the cruise configuration in Fig. 2a accidental. That is, the half-baffled dipole directivity ($\cos^2 \theta / 2$) with no convective amplification assumed by Fink⁴ exactly matches the data of Fig. 3 for $M = 0.441$. These results point out that as yet, no consistent model exists for explaining airframe noise directivity in the cruise configuration. One will be suggested, however, in the course of this paper.

Spectral comparisons were made in the following way. One-third octave band spectra at four aircraft positions (values of θ) along the flight path were selected for comparison with the predicted spectra. The data at the selected angles are typical of the data collected in the neighborhood of those angles along the flight path. The comparisons are shown in Figs. 4a and 4b for the cruise and landing configurations, respectively. The spectra are normalized by their respective predicted or measured OASPL, which may be obtained from Fig. 2. All spectra are to the same scale and have been placed one above the other to facilitate the examination of trends.

In general, the agreement between the measured and predicted spectral shapes is reasonable for both configurations. However, the data are underpredicted at the higher frequencies, particularly for the larger angles. Some of the data may be affected by propagation effects particularly at shallow angles to the ground.

Perhaps the most interesting aspect of Fig. 4 is the double-humped spectra for the cruise configuration. This spectral shape has been observed previously¹² for the 747, Jetstar, and CV990 aircraft, although engine noise was thought to have been an interfering factor. In the DC-9 tests, these double-humped spectra were always observed except for the lower velocity runs and cannot be explained in terms of engine contamination. Treating each hump as a separate source of sound, the levels of these humps may be plotted as a function of the emission angle. These results, corrected to the source location, are shown in Fig. 5. The lower-frequency or first peak is dominant at smaller angles while the reverse is true at the larger angles. The directivity of the first peak appears to follow that of a convected dipole,

$$\bar{p}^2 \sim \frac{\sin^2 \theta}{R^2 (1 - M \cos \theta)^4} \quad (5)$$

which might be expected since at these lower frequencies the wavelength is on the order of or larger than the wing chord.

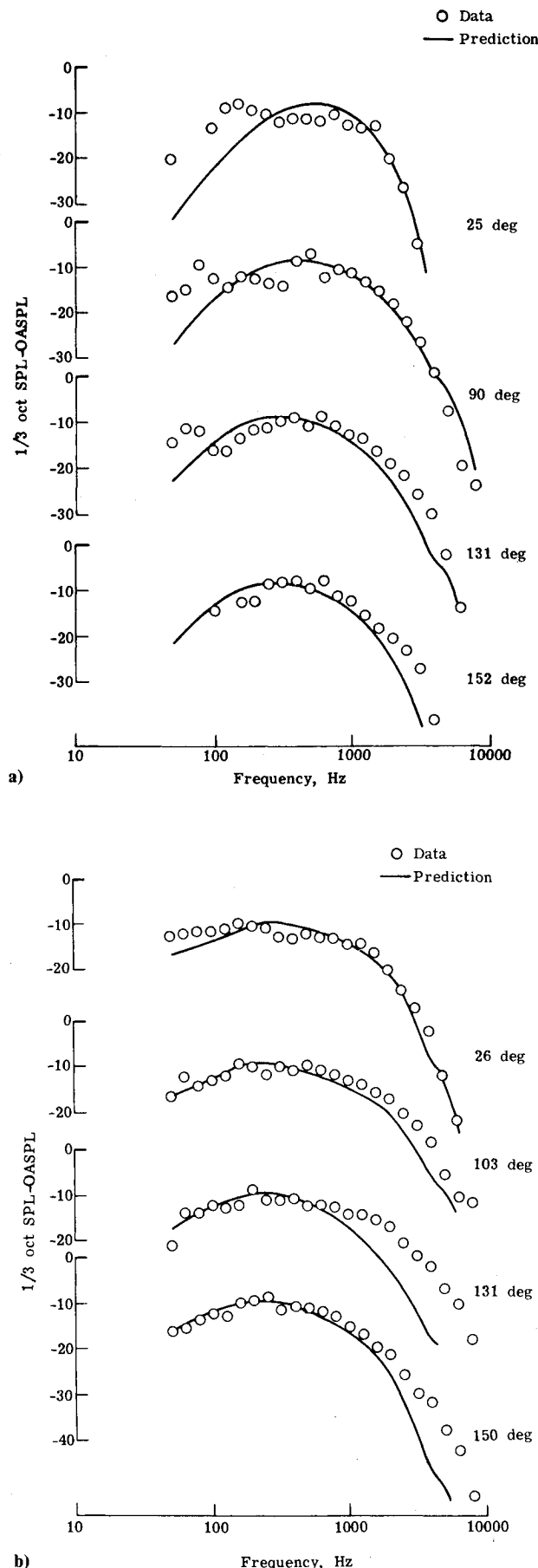


Fig. 4 Comparison of the normalized measured and predicted $1/3$ -octave SPL's for the DC-9 overflight—flyover plane: a) cruise configuration— $V=151$ m/s, $h=231$ m; b) landing configuration— $V=91.2$ m/s, $h=116$ m.

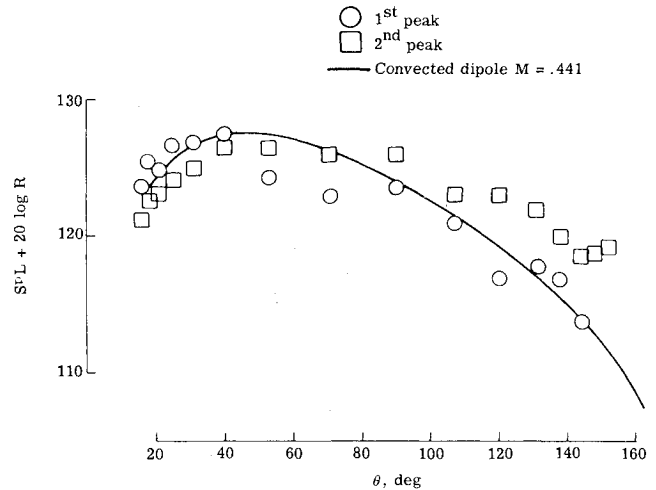


Fig. 5 SPL of the first and second hump of the cruise spectra plotted against flyover angle θ .

Finally, the EPNL's calculated from the data and from the predicted levels for the cases discussed above are shown in Table 1. The rms deviation for the cases examined is about 1 EPNdB. This overall comparison thus indicates that, at least for conventional aircraft, the prediction method is a reasonably accurate means of assessing the impact of airframe noise on the community.

SB-10A Glider Study

The SB-10A is a high-performance glider that was used to study wing and landing gear noise.¹³ This glider has a wing area of 22.9 m^2 and a wing span of 29 m. It was flown at 50 m/s, at 40 m above a microphone on a 5-m pole. Data were corrected to free field in Ref. 13 and are presented in Fig. 6 along with the predicted free field spectral levels. Agreement is fairly good although the peak frequency is lower than that predicted. The peak at about 3 kHz was attributed in Ref. 13 to the horizontal stabilizer as indicated in the figure.

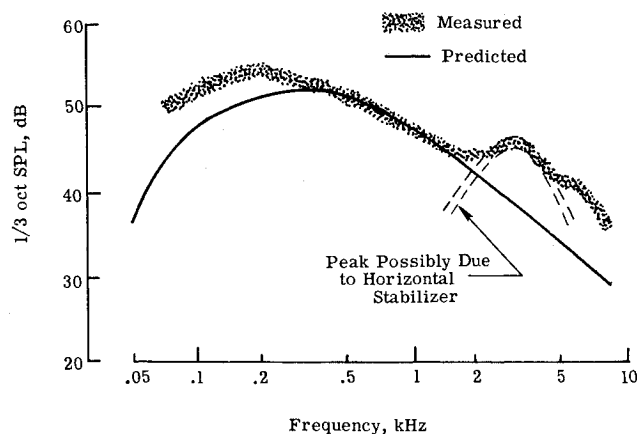
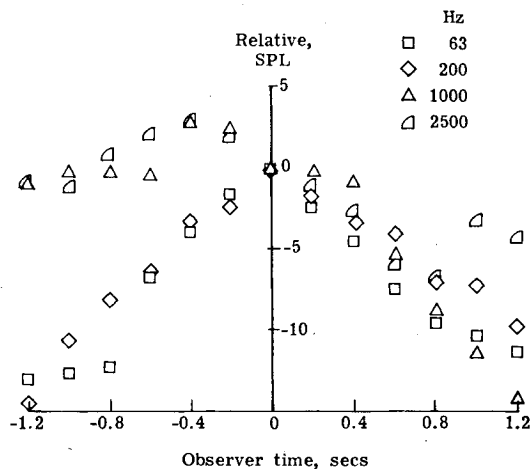
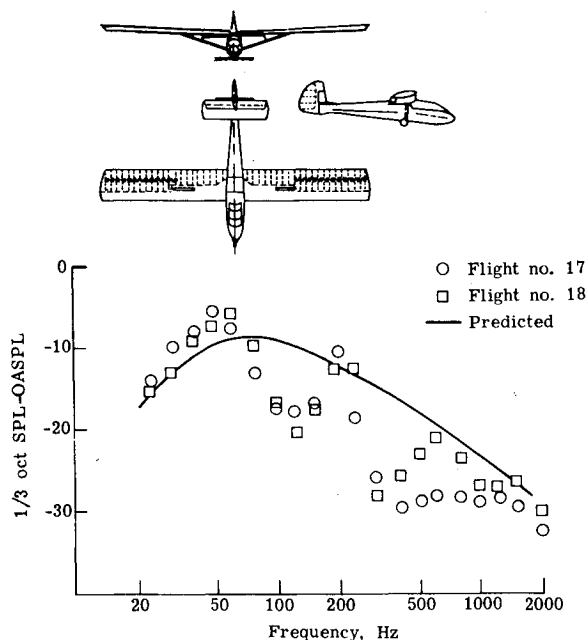
KAI-12 Glider Study

Recently published results from an airframe noise study of two gliders may also be used to exercise the prediction method.¹⁴ The glider with data most pertinent to this study is the KAI-12 glider. The KAI-12 has a wing area of 20.2 m^2 and a wing span of 13.4 m. The altitude of the reported glider overflights ranged from 2 to 45 m over the measurement point and the velocity was nominally 25 m/s. Since only the normalized spectral levels of the flights were provided, the trends will be examined on a normalized level basis by subtracting the predicted OASPL from the predicted spectral levels.

The measured and predicted spectral shapes of the noise for two glider overflights at the same velocity are shown in Fig. 7. The measured spectra are obviously dominated by two rather narrowband components at 63 and 200 Hz. The prediction attempts to pick out the first peak, which is related to the trailing-edge wing noise via Eqs. (3) and (4). However, as in the SB-10 glider, the predicted maximum frequency is somewhat higher than that measured. The predicted spectral shape is broader than that measured for the glider. This is a consequence of constraining the spectral shape or bandwidth of all "trailing-edge" noise to be that of blown flap noise as given by Eq. (2) (see also Fig. 1). Clearly, improvement in the predicted spectral shape will come from a more relevant data base for the clean wing noise. The second spectral peak at 200 Hz coincides with the vortex shedding frequency from a cylinder 3 cm in diameter. This is a reasonable dimension for the wing brace of the KAI-12 glider shown in the inset of Fig. 7, although the tone may arise from the horizontal stabilizer or another source.

Table 1 EPNL's from predicted and measured results for the DC-9 overflights, EPNdB

Configuration	Flyover		152-m sideline		305-m sideline	
	Measured	Predicted	Measured	Predicted	Measured	Predicted
Cruise	88.1	87.2	84.9	85.0	82.2	83.1
Landing	95.1	95.0	88.2	89.7	85.0	87.0

**Fig. 6** Comparison of measured and predicted absolute $\frac{1}{3}$ -octave SPL's for the SB-10A glider: $V = 50$ m/s.**Fig. 8** Variation of four $\frac{1}{3}$ -octave band levels during a KAI-12 glider overflight: $V = 25$ m/s.**Fig. 7** Comparison of measured and predicted relative $\frac{1}{3}$ -octave SPL's for the KAI-12 glider: $V = 25$ m/s.

The directivity of the sound in the 63 Hz, 300 Hz, 1000 Hz, and 2500 Hz $\frac{1}{3}$ -octave bands are shown in Fig. 8.[‡] The peak frequency (63 Hz) and the suspected brace vortex shedding frequency (200 Hz) both display a symmetric dependence on the observer time which suggests a dipole-type source. The 1000-Hz and 2500-Hz bands, however, have higher levels for negative values of the observer time. This behavior suggests a source whose directivity peaks prior to the arrival of the source and, in fact, the half-baffled dipole fits this type of

[‡]The data from Ref. 14 are given in observer time and coordinates. It is not possible to convert source time, since the exact altitude of the overflight is not given. However, assuming a nominal 40-m overflight, the $t = 0$ axis of Fig. 7 would shift 0.1 s to the right when converting to source time.

behavior. These data suggest that the wing has a baffling effect on the noise produced at the trailing edge. The higher frequencies tend toward the half-baffled dipole directivity while the lower frequencies, which dominate the OASPL, show a dipolelike directivity at least for this lower velocity airplane.

0.03 Model 747

Measurements of the airframe noise generated by a model of the Boeing 747 were conducted in a quiet flow facility.¹⁵ The test provided an adequate signal-to-noise ratio with the model in the landing configuration. Grit was applied to wing surfaces to eliminate airfoil tones. The predicted and measured spectra at 90 deg to the airplane axis are shown in Fig. 9. The agreement is certainly satisfactory considering that the semiempirical prediction method uses mostly full-scale data as its base. This result suggests that, within the Reynolds number range of typical model tests and full-scale tests, the relations described in Fig. 1 may be adequate for model predictions as well. This conclusion is supported in part by other model tests.

Model SST

Airframe noise tests of a 0.015-scale model of a proposed supersonic transport were conducted in the NASA Langley ANRL Anechoic Flow Facility.¹⁶ Results from this test are particularly important since little airframe noise data on supersonic design airframes is available.

Predicted and measured directivities for the model in both cruise and landing configuration are shown in Fig. 10. These results have been normalized to a constant radius of 1.6 m. The landing configuration is slightly underpredicted for the smaller angles and more so at the larger angles. The cruise configuration prediction shows no agreement with the data (which is symmetric) other than in the maximum level. However, the data do follow the dipole-like behavior represented by the dashed line in Fig. 10. This dipole has been superimposed over the data such that the dipole axis is normal to the direction of the flow. This gives better agreement than aligning the dipole axis normal to the airframe axis.

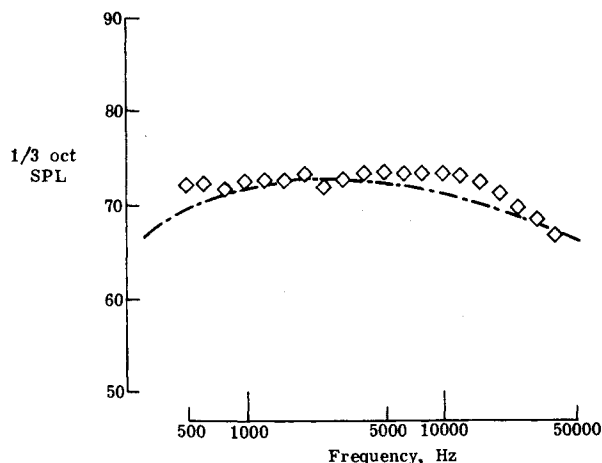


Fig. 9 Comparison of the measured and predicted spectra for the 0.03-model 747 in the landing configuration: $V = 50$ m/s.

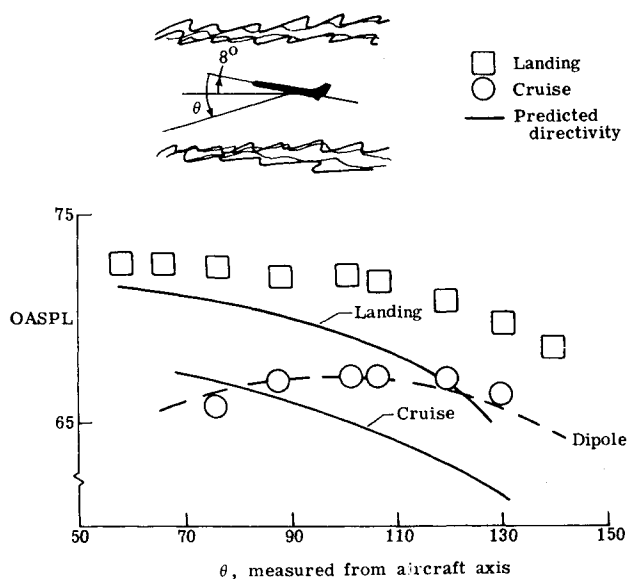


Fig. 10 Measured and predicted OASPL's of the 0.015-model SST: $V = 31$ m/s.

The measured and predicted spectra at 90 deg to the airplane axis are shown in Fig. 11. Considerable agreement in the spectral shape and level can be seen. The difference in SPL's in the landing configuration may be caused in part by the "nonstandard" main landing gear design which consists of 12 wheels per strut. This arrangement cannot be accommodated by the landing gear models of Refs. 4 and 8. The 12 wheels were simulated in the prediction by a single set of four wheels on each side. The effect of the additional eight wheels would be to increase the level and possibly to change the spectral shape. Further acoustic research is needed in order to accommodate the nonconventional designs of proposed aircraft.

Model Spanloader

Airframe noise measurements of a 0.006-scale model of a spanloader transport were made in the NASA Langley ANRL Anechoic Flow Facility. The model, seen in the inset of Fig. 12, had a 16-m chord, 20% thick symmetric airfoil. Grit was applied to the leading edge. In the cruise configuration, the model was aerodynamically very clean. The landing configuration consisted of the clean airfoil, 24 landing gear (covered with grit), four inboard flaps deflected 30 deg, and two outboard flaps deflected minus 15 deg.

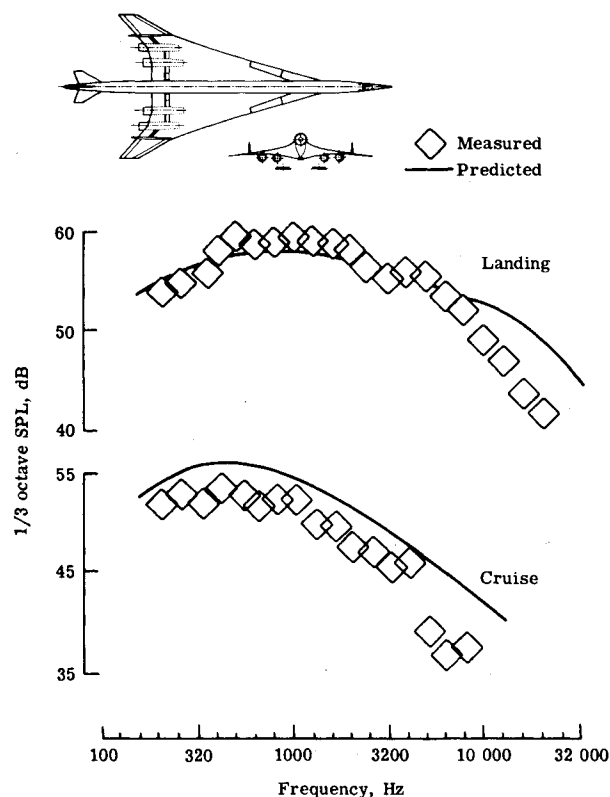


Fig. 11 Comparison of the measured and predicted spectra for the 0.015-model SST: $V = 30$ m/s.

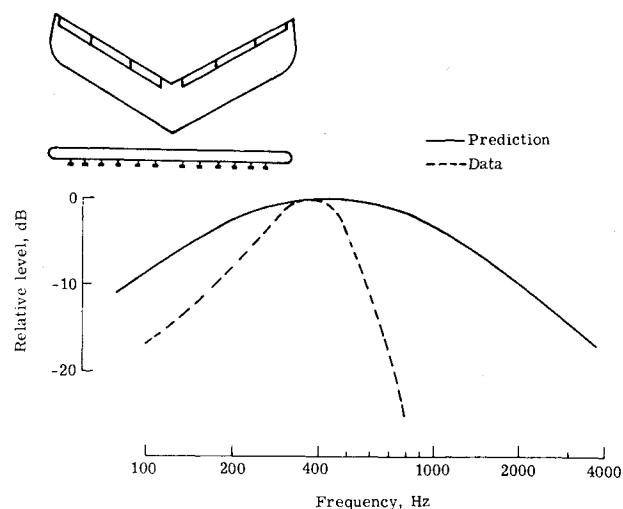


Fig. 12 Comparison of measured and predicted narrowband spectra for the 0.006-model spanloader in the cruise configuration: $V = 35$ m/s.

In the clean configuration where the model is essentially a "flying wing," facility background noise became an interfering factor. To extract the data, two microphones were placed at equal distances above and below the model and the cross spectra were obtained. These results are presented in Fig. 12 over the frequency range where the signals were coherent. Also presented is the predicted spectral shape for the clean configuration. The predicted peak frequency is slightly higher (as in the case of the gliders) but the predicted spectral width is much greater than that of the data.

Discussion of Results

In general, the FAA component method has provided a fairly consistent estimate of the airframe noise of a wide

Table 2 Some aircraft parameters used to predict the EPNL for operational and proposed aircraft

Aircraft	S_w, m^2	b_w, m	S_{flap}, m^2	chord _{flap} , m	δ_f, deg	$V, m/s$
DC-9	92.97	28.47	19.58	.898	45	64.4
B-727	157.9	32.92	36.	1.8	30	64.8
A-300-B2	260.	44.8	46.8	1.45	45	67.9
Concorde SST	385.25	25.56	32.0	1.78	45	89.6
L1011	320.	47.34	49.8	1.91	45	73.3
DC-10	367.7	50.4	62.1	2.13	45	70.6
B-747	511.	56.64	78.7	2.7	45	72.4
Space Shuttle	250.	23.8	161.5	2.2	15	90.
LFC	444.4	67.05	74.3	1.37	25	69.5
AST-100	1021.	42.	80.2	4.32	20	81.8
Spanloader	3784.	153.3	656.8	4.17	45	77.2

variety of aircraft of wing spans from less than 1 to 30 m. However, certain observations may be collected and noted.

Directivity

The prediction does not include convective amplification effects. These effects are observable and perhaps ought to be incorporated for higher-velocity aircraft as evidenced by the change in the DC-9 cruise directivity with forward velocity (see Fig. 3). However, at lower velocities (glider and model tests), these effects can be neglected without clouding the discussion of the actual source directivity.

The cruise results of this study indicate that the shape of the directivity is determined by the ratio of the wavelength of the major sound source to the chord dimension. When this ratio is large (as is the case for the glider, the models, and the first peak in the DC-9 cruise spectra) a dipole directivity is measured. The data from the latter agrees with a convected dipole shape [Eq. (5)]. The symmetric behavior of the glider and model directivities also lead to the conclusion of an un baffled or free dipole source. When the wavelength is less than or on the order of the chord dimension, diffraction effects can be expected. The magnitude of these effects is not known at present except for the case where the wavelength is much less than the chord. In this case the half-baffled dipole is applicable. For conventional aircraft at typical approach velocities, the predicted wavelength (c/f_m) suggests that an un baffled or free dipole is a more appropriate model for the cruise directivity. Strictly speaking, only at very high frequencies (or high approach velocities coupled with large chord dimension) would one expect to observe the half-baffled dipole as predicted by Ref. 6.

The predicted variation of the OASPL with the flyover angle θ gave good agreement with data in the landing configurations where the flap and landing gear are the dominant noise sources. This configuration is the basis for the comparison with noise regulations.

Spectra

The predicted peak frequency for the cruise spectra was slightly higher than that measured for all of the data presented herein. The predicted cruise spectral shape is too broad for the low-velocity simpler aerodynamic designs such as the KAI-12 glider (Fig. 7) and spanloader (Fig. 12). These simple clean configurations apparently do not generate the higher frequencies of the more detailed SST and DC-9 airframes or the higher-velocity SB-10 glider. Improvement would permit the peak frequency and bandwidth to be dependent on design and velocity.

The good agreement in the landing condition, where the flaps and landing gear are usually the primary sources (Figs. 2b, 4b, 9, 11), suggests that the current modeling of the flaps and landing gear (see Fig. 1) is reasonably adequate. Improved models would make this prediction method more consistent but would probably not significantly affect the predictions of the EPNL. However, improved models can provide insight into possible noise reduction measures.

Level

The predicted and measured levels agreed very well with the full-scale DC-9 tests. The model tests give inconsistent results. However, the predicted levels are always within a few decibels of the measured levels for each of the models, even though they vary drastically in design. Since the spectral peak and levels agree fairly well with model results, scaling on dimension and velocity appears to be a valid and appropriate procedure for estimating full-scale levels from model scale results providing the flow simulation is realistic. The comparison of the EPNL's from the DC-9 test indicate that the FAA component method produces a good estimate of annoyance due to the airframe noise.

Estimation of EPNL

The ability of the component method to predict the spectra and directivity of airframe noise in the landing configuration as shown by the foregoing work, justifies its utilization to estimate the contribution of airframe noise to community noise levels. These levels are predicted for both operational and proposed aircraft. A note of caution must be added at this point: since the proposed design airplanes vary significantly from the designs on which this prediction method was generated, the estimates must be considered as initial estimates which result from current predictive technology.

A sample of important aircraft parameters that were used in the prediction is given in Table 2. The observer location is the FAR-36 point for landing approach, and standard atmospheric conditions were used. All aircraft were assumed to follow a 3-deg glide slope with the approach velocity given in Table 2.

Conventional Design Airplanes

The current noise regulations and certification levels¹⁷ are shown in Fig. 13. Also shown are the predicted airframe noise EPNL's of several commercial fleet airplanes in the landing configuration. The higher level assigned to the 727 and the 747 is attributed to the high-frequency contribution of the triple-slotted trailing-edge flap design (see Fig. 1). This design has been found empirically to generate high-frequency noise⁴ which is considered more annoying and which is consequently reflected in the calculation of the EPNL. The Concorde airplane has a higher approach speed (about 90 m/s) and thus a higher value of OASPL and consequently of EPNL than the other airplanes of similar weight.

In general, operational airframe noise levels are about 10 EPNdB below present certification levels and the current noise regulations. The predicted EPNL's of these aircraft in the cruise configuration (not shown) are 20 EPNdB below current noise regulations.

Advanced Design Airplanes

The predicted EPNL's for aircraft that may appear in the next several decades are indicated by the shaded symbols on Fig. 13. The Space Shuttle EPNL is predicted to be of higher level than airplanes of similar weight because of the high

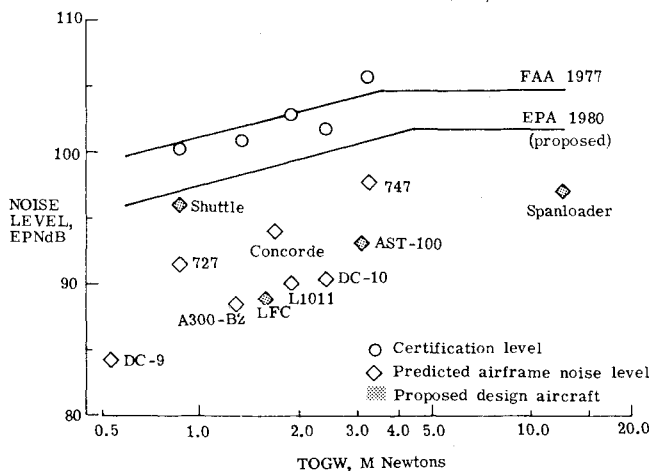


Fig. 13 Comparison of noise regulations with predicted airframe noise levels.

approach speed of 90 m/s and large flap area. However, it is not presently anticipated that the Space Shuttle will use airports in densely populated areas.

The Laminar Flow Control (LFC) airplane is designed to be a fuel-efficient transport. The predicted EPNL for the landing approach lies in the range of other aircraft of similar weight. Since the landing approach operation and configuration will not be unlike that of the current fleet, the predicted level shown in Fig. 13 is considered realistic.

The Advanced Supersonic Transport (AST-100) is predicted to have slightly less annoying airframe noise levels than the Concorde SST. Although larger than the Concorde SST, the low design approach speed (82 m/s) for this aircraft gives a lower airframe noise level.

The Spanloader is a cargo transport reminiscent of the flying wing. Despite its large takeoff gross weight, it is predicted to be less annoying than a 747. This stems from the fact that the major noise contribution of the spanloader is in the lower frequencies which are not presently considered annoying.

Conclusions

From the foregoing analysis, the following conclusions may be drawn:

1) The FAA Component Method developed by Fink⁴ is consistent in predicting airframe noise levels for both model- and full-scale airplanes.

2) The trailing-edge wing noise for typical aircraft at the lower approach speeds appears to have a free dipole directivity as opposed to a half-baffled dipole directivity pattern.

3) Predicted airframe noise levels for current aircraft designs are about 10 EPNdB below current noise regulations. The first estimates of proposed aircraft EPNL's do not indicate significant contribution of airframe noise to community noise levels.

References

- Revell, J.D., Healy, G.J., and Gibson, J.S., "Methods for the Prediction of Airframe Aerodynamic Noise," AIAA Paper 75-539, Hampton, Va., March 1975.
- Munson, A.G., "A Modeling Approach to Nonpropulsion Noise," AIAA Paper 76-525, Palo Alto, Calif., July 1976.
- Hardin, J.C., Fratello, D.J., Hayden, R.F., Kadman, Y., and Africk, S., "Prediction of Airframe Noise," NASA TN-D 7821, Feb. 1975.
- Fink, M.R., "Airframe Noise Prediction Method," Final Report for U.S. Department of Transportation, FAA-RD-77-29, March 1977.
- Fink, M.R. and Schlinker, R.H., "Airframe Noise Component Interaction Studies," NASA CR 3110, March 1979.
- Ffowcs-Williams, J.E. and Hall, L.H., "Aerodynamic Sound Generation by Turbulent Flow in the Vicinity of a Scattering Half Plane," *Journal of Fluid Mechanics*, Vol. 40, March 1970, pp. 657-670.
- Private communication with Martin Fink, Nov. 1978.
- Heller, H.H. and Dobrzynski, W.M., "Sound Radiation from Aircraft Wheel-Well/Landing Gear Configurations," AIAA Paper 76-552, Palo Alto, Calif., July 1976.
- Dobrzynski, W.M. and Heller, H.H., "Are Wheel-Well Aeroacoustic Sources of Any Significance in Airframe Noise?" AIAA Paper 77-1270, Atlanta, Ga., Oct. 1977.
- Raney, J.P., "Noise Prediction Technology for CTOL Aircraft," *Proceedings of the CTOL Transport Technology Conference*, NASA CP-2036, 1978.
- Bauer, A.B. and Munson, A.G., "Airframe Noise of the DC-9-31," AIAA Paper 77-1272, Atlanta, Ga., Oct. 1977; also NASA CR 3027.
- Putnam, T.W., Lasagna, P.L., and White, K.C., "Measurements and Analysis of Aircraft Airframe Noise," AIAA Paper 75-510, Hampton, Va., March 1975.
- Heller, H.H. and Dobrzynski, W.M., "Unsteady Surface Pressure Characteristics on Aircraft Components and Farfield Radiated Airframe Noise," *Journal of Aircraft*, Vol. 15, Dec. 1978, pp. 809-815.
- Vlasov, E.V. and Samokhin, V.F., "Aerodynamic Noise of Gliders," *Society Physical Acoustics*, Vol. 23, July-Aug. 1977, pp. 314-318.
- Shearin, J.G., Fratello, D.J., Bohn, A.J., and Burggraf, W.D., "Model and Full Scale Large Transport Airframe Noise," AIAA Paper 76-550, Palo Alto, Calif., July 1976.
- Preisser, J.S., "Airframe Noise Measurements of a Small-Scale Model of a Supersonic Transport Concept in an Anechoic Flow Facility," AIAA Paper 79-0666, Seattle, Wash., March 1979.
- Jane's All the World's Aircraft*, Jane's Yearbooks, London, 1977/78.